vain, Louvain, France, 1964); V. S. Ramachandran, in *The Perception of Illusory Contours*, G. E. Petry and S. Meyer, Eds. (Springer-Verlag, Berlin, 1987), pp. 93–108; T. F. Shipley and P. J. Kellman, *J. Exp. Psychol. Hum. Percept. Perform.* **18**, 106 (1992).
10. Z. J. He and K. Nakayama, *Nature* **359**, 231 (1992); J. T. Enns and R. A. Rensink, in *Visual Search III: Proceedings of the Third International Conference on Visual Search*, A. G. Gale, Ed. (Taylor and Francis, London, 1994); G. Davis and J. Driver, *Nature* **371**, 79 (1994).
11. B. T. Volpe, J. E. Le Doux, M. S. Gazzaniga, *Nature* **282**, 722 (1979); J. C. Marshall and P. W. Halligan, *ibid.* **336**, 766 (1988); A. Berti and G. Rizzolatti, *J. Cogn. Neurosci.* **4**, 345 (1992); E. Làdavas, R. Paladini, R. Cubelli, *Neuropsychologia* **31**, 1307 (1993).
12. Z. J. He and K. Nakayama, *Proc. Natl. Acad. Sci. U.S.A.* **92**, 11155 (1995); K. Nakayama, Z. J. He, S. Shimojo, in *An Invitation to Cognitive Science (2nd Ed)–Visual Cognition (Vol. 2)*, S. M. Kosslyn and D. N. Osherson, Eds. (MIT Press, Cambridge, MA, 1995), pp. 1–70.
13. For several reasons, V.R. is an ideal case for testing our hypothesis that the processes underlying visual filling-in will remain intact in parietal extinction. First, her lesion is primarily cortical, but she has no visual field cuts. The clinical phenomenon of extinction can be observed in several kinds of neurological patients but may arise for different reasons after the occurrence of distinct lesions [such as partial sensory loss (*4*) in patients with subcortical lesions]. Patients with mainly cortical damage (like V.R.) show deficits that are more attentional in nature and therefore provide the critical test for our present hypothesis; however, unlike V.R., many cortical patients have visual field cuts that render them unsuitable for our tests. Second, the large extent of V.R.'s cortical lesion places considerable constraints on the neural substrate for the preserved visual filling-in that we find within the intact tissue. Finally, although extinction is relatively common for a brief period after unilateral brain damage, it is often transient. In this respect, V.R. is also a particularly useful case; her disorder remained stable over many months, permitting the extensive testing documented here.
14. R. Ward, S. Goodrich, J. Driver, *Visual Cogn.* **1**, 101 (1994).
15. R. von der Heydt, E. Peterhans, G. Baumgartner, *Science* **224**, 1260 (1984); R. von der Heydt and E. Peterhans, *J. Neurosci.* **9**, 1731 (1989).
16. R. Jackendoff, *Consciousness and the Computational Mind* (MIT Press, Cambridge, MA, 1987).
17. V.R.'s small left-hemisphere lesion had occurred 2 years before the right-hemisphere stroke, causing a transient right-sided homonymous hemianopia which resolved completely and no other symptoms. At the time of the present investigations, V.R. had full visual fields. There was no evidence of unilateral left neglect when conventional measures were used, including line-bisection and cancellation tasks; but V.R. showed consistent extinction of contralesional stimuli in the visual, tactile, and auditory modalities on confrontation. The experiments reported here were conducted between 1 and 24 months after the right-hemisphere stroke.
18. All stimuli were displayed on the active matrix screen of a Macintosh PowerBook 540, controlled by VScope software [J. T. Enns and R. A. Rensink, *VScope Software Manual: Vision Testing Software for the Macintosh* (Micropsych Software, University of British Columbia, Vancouver, Canada, 1992)]. The viewing distance was 50 cm. Circular inducers were 5.1° in diameter, with a center-to-center separation of 10.2° horizontally and 7.4° vertically (all drawings are to scale, so that other visual angles may be derived).
19. The duration for which the target segments were removed was determined before each experiment by a titration procedure aimed at producing 75% correct detections for unilateral left trials. This duration was 500 ms in experiment 1, 100 ms in experiment 2, and 250 ms in experiment 3.
20. Within each experiment, all the conditions were implemented during a single session and in counterbalanced order, to rule out any influences of practice or long-term recovery on the comparisons of interest.
21. In experiments 1, 3, and 4, V.R. completed four blocks of 36 trials, the two possible display types being blocked with their order counterbalanced in an ABBA design. In experiment 2, V.R. completed six blocks of 36 trials in an ABBAAB design. Each block always contained 16 bilateral, 8 unilateral left, and 8 unilateral right trials for a particular display type, plus 4 catch trials, all in a random order.
22. In experiment 1, V.R. detected 12 out of 16 (12/16) unilateral left events and 15/16 unilateral right events of the inner type; and 15/16 unilateral left plus 16/16 unilateral right events of the outer type. She correctly reported the absence of any target event on all catch trials. In experiment 2, V.R. detected 23/24 unilateral left events and 24/24 unilateral right events for left-inner displays; and 24/24 unilateral events (left and right) for left-outer displays. For both display types in experiment 3, she detected 16/16 unilateral events (left and right), and made no false-positive responses on catch trials; likewise for experiment 4.
23. The sequence of events in each trial was similar to that in experiments 1 through 4. A central fixation cross was displayed for 500 ms. This was replaced by a pictured cube (maximum height 10.8°, maximum width 14.6°) with perspective and shading cues constructed to yield a 3D shape. The "nearest" vertical edge of the cube appeared at the center of the screen, in line with fixation. One second later, a black horizontal bar appeared for 150 ms to the left or right of the cube (unilateral trials); or two bars appeared simultaneously for 150 ms on either side (bilateral trials, as illustrated); or no bars appeared (catch trials). The cube remained visible until V.R. reported whether there had been any bar on the right, left, both sides, or neither side. Each block of trials had the same structure as previously. The three display types were blocked in an ABCCBA order.
24. For all three display types in experiment 5, V.R. detected every unilateral stimulus on the left and right and correctly reported the absence of any bars on all catch trials.
25. We thank V.R. for her willing participation. J.B.M. was supported by a National Health and Medical Research Council (Australia) Neil Hamilton Fairley Fellowship, G.D. by the Biotechnology and Biological Sciences Research Council (UK), and J.D. by the Wellcome Trust (UK). We thank J. Bradshaw, J. Duncan, J. Pierson, I. Robertson, C. Rorden, and S. Tripathy for comments on the manuscript.

2 August 1996; accepted 26 November 1996

NMDA Channel Regulation by Channel-Associated Protein Tyrosine Kinase Src

Xian-Min Yu, Rand Askalan, Gary J. Keil II, Michael W. Salter*

The *N*-methyl-D-aspartate (NMDA) receptor mediates synaptic transmission and plasticity in the central nervous system (CNS) and is regulated by tyrosine phosphorylation. In membrane patches excised from mammalian central neurons, the endogenous tyrosine kinase Src was shown to regulate the activity of NMDA channels. The action of Src required a sequence [Src(40–58)] within the noncatalytic, unique domain of Src. In addition, Src coprecipitated with NMDA receptor proteins. Finally, endogenous Src regulated the function of NMDA receptors at synapses. Thus, NMDA receptor regulation by Src may be important in development, plasticity, and pathology in the CNS.

The NMDA receptor is a principal subtype of ionotropic excitatory amino acid receptor that plays a central role in development, neuroplasticity, and excitotoxicity in the CNS (*1*). The function of NMDA receptor is regulated by protein phosphorylation at serine or threonine (*2*) and at tyrosine (*3*, *4*) residues. For serine or threonine kinases, protein kinase C is an endogenous kinase (*5*) that regulates NMDA channel function. In contrast, the endogenous tyrosine kinase that regulates NMDA channels has been elusive. Numerous receptor (*6*), as well as nonreceptor (*7*), tyrosine kinases are expressed in the CNS. We set out to identify the endogenous tyrosine kinase regulating NMDA channel function.

We recorded NMDA receptor single-channel currents using inside-out patches taken from cultured rat central neurons (*8*). To investigate whether the endogenous tyrosine kinase was a nonreceptor tyrosine kinase in the Src family, we made use of a high-affinity peptide, EPQ(pY)EEIPIA (*9*), which activates this family of kinases. The nonphosphorylated form of the peptide, EPQYEEIPIA, is inactive (*9*) and was used as a control. Application of EPQ(pY)-EEIPIA to the cytoplasmic side of the membrane produced an increase in the channel activity (*10*) while having no effect on single-channel conductance (Fig. 1A). On average, channel open probability (P_o) increased to 260 ± 38% of the control value (mean ± SEM; n = 7 patches), and there was an increase in mean open time to 152 ± 18%. Peptide EPQ(pY)EEIPIA caused marked changes in the distribution of open and shut times (Fig. 1A), with alterations in the relative area of the components and no significant changes in the values of the time constants. In the distribution of open times, the area of the longest component was increased. For shut times, the area of the shortest component increased and that of the longest component decreased. Peptide EPQ(pY)EEIPIA also

Division of Neuroscience, Hospital for Sick Children, Department of Physiology, University of Toronto, Toronto, Ontario, M5G 1X8 Canada.

*To whom correspondence should be addressed. E-mail: mike.salter@utoronto.ca

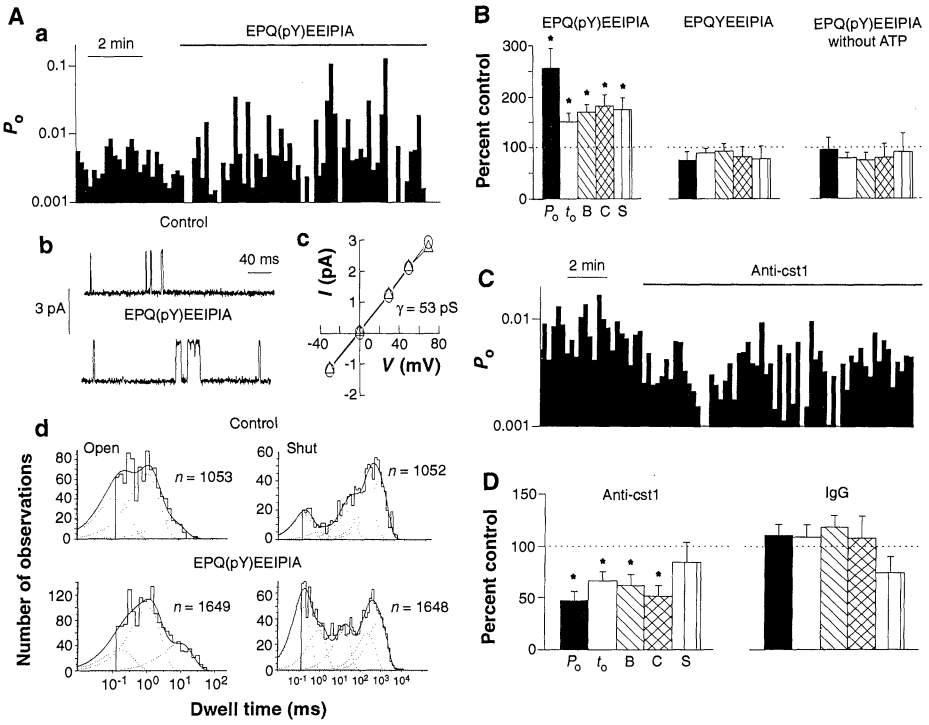

Fig. 1. Modulation of NMDA channel activity by a peptide activator or an antibody inhibitor of Src family kinases. (**Aa**) A continuous record of NMDA channel open probability (P_o) before and during cytoplasmic application of EPQ(pY)EEIPIA (1 mM; bar). NMDA channel P_o was calculated in bins 10 s in duration. (**Ab**) Single-channel currents before (Control; upper trace) and during (lower trace) application of EPQ-(pY)EEIPIA. (**Ac**) Current-voltage (*I-V*) relation for mean NMDA single-channel currents before (circles) and during (triangles) application of EPQ(pY)EEIPIA. (**Ad**) Dwell-time histograms of open and shut times before (upper panels) and during (lower panels) application of EPQ(pY)EEIPIA. In this and all other dwell-time histograms the dashed lines indicate individual exponential components, the solid line shows the sum of the components, and *n* is the number of events. The average time constants of the components (±SEM) were 0.12 ± 0.05, 0.98 ± 0.45, and 3.0 ± 0.9 ms (open times) and 0.15 ± 0.02, 1.7 ± 0.27, 26 ± 4.0, 380 ± 86, and 1700 ± 540 ms (shut times), before peptide administration (n = 7 patches). (**B**) Effect of EPQ(pY)EEIPIA (n = 7), EPQYEEIPIA (1 mM; n = 5 patches), and EPQ(pY)EEIPIA, in the absence of ATP (n = 5 patches), on NMDA channel activity. Values are the means ± SEM. The dashed line indicates control values before peptide application [P_o and mean open time = (3.7 ± 0.9) × 10^{-3} and 2.0 ± 0.5 ms, respectively, and the duration of the bursts, clusters, and superclusters = 2.7 ± 0.8, 9.1 ± 1.7, and 203 ± 41 ms, respectively]. t_o, mean open time; B, burst length; C, cluster length; S, supercluster length. (**C**) A continuous record of the NMDA channel P_o before and during application of anti-cst1 (10 μg/ml; bar). (**D**) Effect of anti-cst1 (n = 6 patches) or the nonselective IgG fraction (10 μg/ml; n = 4 patches) on activity of NMDA channels. *P < 0.05 [Mann-Whitney test for EPQ(pY)EEIPIA versus EPQYEEIPIA, or anti-cst1 versus the nonselective IgG fraction].

produced a significant increase in the duration of the bursts, clusters, and superclusters (Fig. 1B) and in the numbers of openings and mean total open time during the groupings (*11*). In contrast, control peptide EPQYEEIPIA had no significant effect on any of the parameters measured (Fig. 1B) (n = 5 patches). Omitting adenosine 5′-triphosphate (ATP) prevented the effects of EPQ(pY)EEIPIA, consistent with an action due to phosphorylation (Fig. 1B).

In a complementary series of experiments we used an antibody, anti-cst1 (*12*), which inhibits Src family kinases (*13*) (Fig. 1, C and D). Anti-cst1 (10 μg/ml; n = 6 patches) produced significant decreases in P_o, mean open time, and burst and cluster duration (Fig. 1D). In addition, the numbers of openings and mean total open time in all of the groupings were decreased (*11*). In contrast, application of nonselective immunoglobulin G (IgG) fraction (10 μg/ml) had no significant effect (n = 4 patches). The effects of EPQ(pY)EEIPIA and anti-cst1 implied that a Src family kinase was present in the membrane patches and regulated NMDA channel gating.

To determine whether the endogenous kinase was Src itself, we studied the effects of anti-src1 (Fig. 2, A and B) (n = 6 patches), which blocks selectively the function of this kinase (*13*). Administration of anti-src1 decreased NMDA channel gating with no change in single-channel conduc-

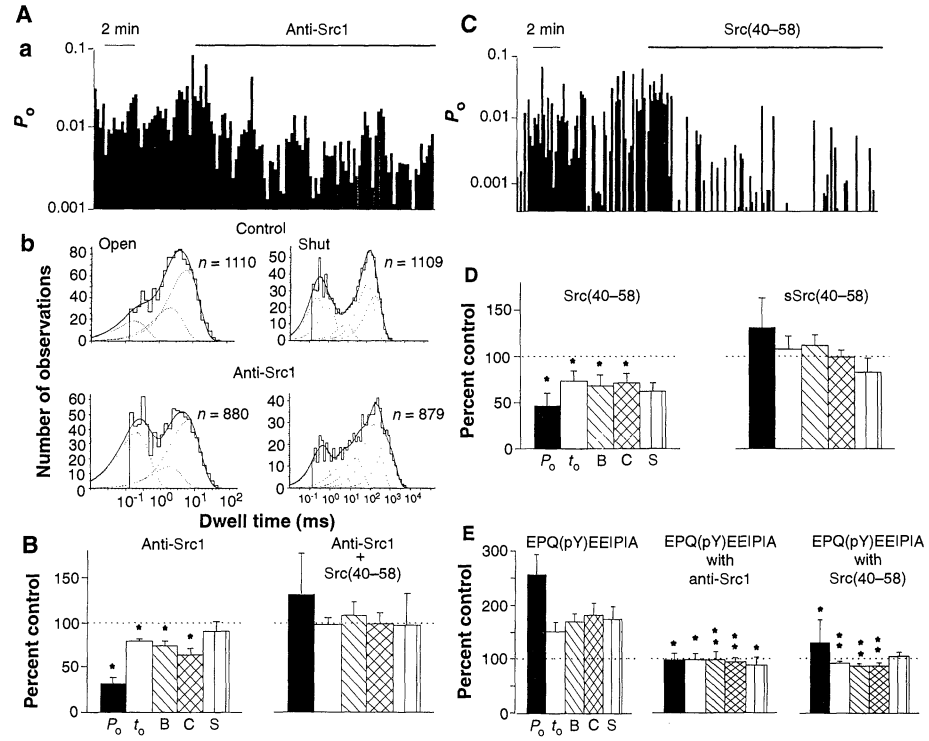

Fig. 2. Regulation of NMDA channel gating by endogenous Src. (**Aa**) A continuous record of NMDA channel P_o in the absence or presence of anti-src1 (1:100 dilution; bar). (**Ab**) Dwell-time histograms of NMDA channel open and shut times before (upper panels) or during (lower panel) application of anti-src1. (**B**) Effect of anti-src1 (mean ± SEM; n = 7 patches) or anti-src1 after incubation with Src(40–58) (n = 3 patches). (**C**) A continuous record of NMDA channel P_o in the absence or presence of Src(40–58) (0.03 mg/ml; bar). (**D**) Effect of Src(40–58) (n = 7 patches) or sSrc(40–58) (0.03 mg/ml; n = 5 patches). (**E**) Effect of EPQ(pY) EEIPIA alone, EPQ(pY)EEIPIA with anti-src1 (n = 5 patches), or EPQ(pY)EEIPIA with Src(40–58) (n = 4 patches) on NMDA channel activity. *P < 0.05 and **P < 0.01 (Mann-Whitney test).

tance: P_o, mean open time, and burst and cluster length were significantly reduced, and the open-time distribution was shifted toward shorter openings and the shut times toward longer closings. The effects of anti-src1 were prevented when it was incubated with the corresponding immunogen peptide, Src(40–58), for 30 min just before use (n = 3 patches). Moreover, EPQ(pY)EEIPIA had no effect when applied to patches that had first been treated with anti-src1 (Fig. 2E) (n = 5 patches). In addition, application of recombinant pp60$^{c\text{-}src}$ (1 U/ml; n = 6 patches) increased P_o to 257 ± 100% of control, mean open time to 125 ± 10%, burst length to 186 ± 23%, and cluster length to 220 ± 33%. These effects were prevented by boiling pp60$^{c\text{-}src}$ to heat-inactivate it just before use (n = 4 patches). Together, these results indicated that NMDA channels were regulated by endogenous Src.

It is possible that anti-src1 acted by preventing an interaction between the region in Src specific for the antibody and a complementary region in a target protein. To investigate this possibility, we studied the effects of Src(40–58) (Fig. 2, C and D). P_o, mean open time, and duration, number of openings, and mean total open time during bursts and clusters were reduced by application of Src(40–58) (n = 7 patches). To control for length, net charge, and amino acid composition, we tested a peptide in which the amino acid sequence of Src(40–58) was scrambled (*8*). Scrambled Src(40–58) [sSrc(40–58)] had no effect on single-channel activity (Fig. 2D) (n = 5 patches). In other experiments, initial treatment with Src(40–58) prevented the effects of EPQ(pY)EEIPIA (Fig. 2E), but these effects persisted with sSrc(40–58) (n = 3 patches). Thus, an interaction between the region of Src(40–58), which is within the unique domain of Src, and another protein may be necessary for the effects of Src on NMDA channels.

To determine whether Src and NMDA channels are associated physically, we immunoprecipitated membrane proteins (*14*) with antibodies specific for the NR1 subunit of NMDA receptors (anti-NR1) or for Src (anti-Src). When we used nondenaturing conditions (*15*) to solubilize membrane proteins, immunoprecipation with anti-NR1 resulted in coprecipitation of Src (Fig. 3A). Conversely, immunoprecipitation with anti-Src resulted in coprecipitation of NR1 (Fig. 3B). In contrast, the K^+ channel protein Kv3.1 (*16*) was not immunoprecipitated either by anti-Src or anti-NR1, indicating that precipitation of membrane pro-

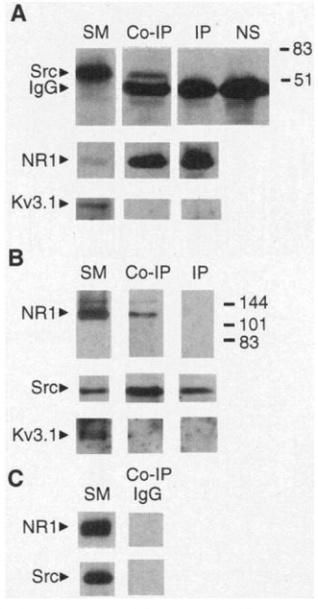

Fig. 3. Association of Src and NMDA channel proteins. Immunoprecipitation with anti-NR1 (**A**) and anti-Src (**B**), or nonspecific IgG (**C**). Membrane proteins were solubilized under nondenaturing (Co-IP) or under denaturing conditions (IP). Proteins were resolved by SDS-PAGE, transferred to nitrocellulose, and analyzed by sequential immunoblotting with anti-NR1, anti-Src, or anti-Kv3.1 as indicated. SM, lanes loaded with 50 μg of solubilized membranes without immunoprecipitation; NS, lane loaded with antibody but no sample to demonstrate the position of the IgG heavy chain. Molecular size standards (in kilodaltons) are indicated on the right. The results are representative of five (A), six (B), or three experiments (C).

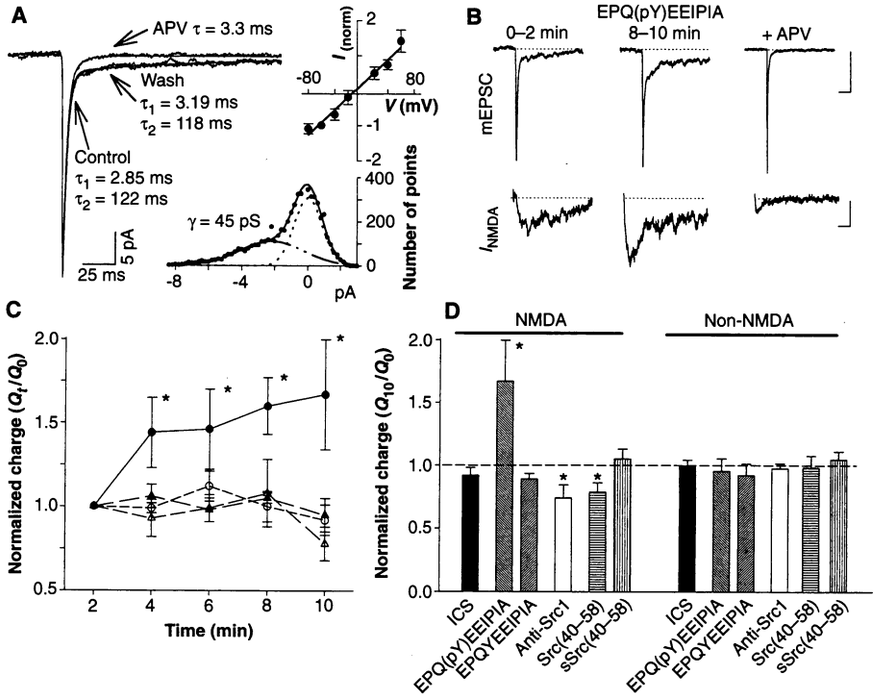

Fig. 4. Regulation of synaptic NMDA currents by endogenous Src. (**A**) Representative recording of averaged mEPSCs before (Control) or during application of APV (100 μM), and after wash; τ, decay time constants of the currents. (**Inset**) (Top) The *I-V* plot of the NMDA component of averaged mEPSCs. Each point is the mean of the amplitude of the NMDA component (±SEM; n = 6 cells) relative to those recorded at −60 mV [$I_{(norm)}$]. (Bottom) An all-points distribution histogram of current 60 to 90 ms after the start of 20 consecutive mEPSCs. The distribution was fit as the sum of two Gaussian curves (solid line). One peak occurred at −0.1 pA and represented background noise. The other peak was at −2.7 pA, from which a single-channel conductance was calculated. (**B**) A representative recording of averaged mEPSCs (top traces) or NMDA components (I_{NMDA}) (bottom traces) compiled immediately after breakthrough (0 to 2 min), 8 to 10 min later, and during bath application of APV (100 μM) when EPQ(pY)EEIPIA (1 mM) was included in the recording pipette. We constructed I_{NMDA} by subtracting, from the averaged mEPSC, a current decaying at a single exponential rate equal to the fast component. Bars: time, 25 ms; current, 5 pA (top) and 2 pA (bottom). (**C**) NMDA and non-NMDA synaptic responses during recordings with EPQ(pY)EEIPIA (1 mM, closed symbols; n = 8 cells) or EPQYEEIPIA (1 mM, open symbols; n = 5 cells). We calculated charge (Q) by integrating currents during NMDA (circles) or non-NMDA (triangles) components of mEPSCs. For each cell, charge during consecutive 2-min periods (Q_t) was normalized to that measured during the initial 2-min period (Q_0). (**D**) Mean Q_{10}/Q_0 for NMDA or non-NMDA components. Recordings were done with intracellular solution (ICS; n = 5 cells) or intracellular application of EPQ(pY)EEIPIA, EPQYEEIPIA, anti-src1 (1:100 dilution; n = 6 cells), Src(40–58) (0.03 mg/ml; n = 7 cells), or sSrc(40–58) (0.03 mg/ml; n = 6 cells). (C and D) *P < 0.05, paired t test.

teins did not occur nonspecifically. The coprecipitation of Src by anti-NR1 and of NR1 by anti-Src was prevented when denaturing solubilization conditions were used, whereas the immunoprecipitation of NR1 or Src by the corresponding antibodies was not affected. Moreover, neither NR1 nor Src was precipitated by nonspecific IgG. Thus, Src may have been physically associated with NMDA channels in vitro.

To investigate whether synaptic NMDA receptors were regulated by Src (*17*), we studied miniature excitatory postsynaptic currents (mEPSCs). These mEPSCs showed NMDA- and non-NMDA receptor–mediated components (Fig. 4A) (*18*). Intracellular administration of EPQ(pY)EEIPIA increased the average NMDA component of the mEPSCs to ~160% of the initial value (Fig. 4, B and C) (n = 8 cells). During the recording period there was no change in reversal potential, indicating that there was no alteration of driving force (*11*). In contrast to recordings with EPQ(pY)EEIPIA, the NMDA component was unaffected when EPQYEEIPIA was administered (n = 5 cells). In other recordings, addition of anti-src1 or Src(40–58) significantly reduced the NMDA component of the mEPSCs, whereas sSrc(40–58) had no effect (Fig. 4D). The non-NMDA component of the mEPSCs was unaffected by EPQ(pY)EEIPIA, EPQYEEIPIA, anti-Src1 (n = 6 cells), Src(40–58) (n = 7 cells), or sSrc(40–58) (n = 6 cells). The non-NMDA channels studied in this way were located at the same synapses as the NMDA channels (*18*); thus, even within the restricted space of a single postsynaptic site, Src appeared to regulate NMDA but not non-NMDA channels.

Src is expressed at high levels in the CNS and is found preferentially in neurons that express an alternatively spliced form of the enzyme (*7*). However, the functions of Src in the CNS have until now remained enigmatic (*19*). These results indicate that Src may be a member of the NMDA channel complex and that one function of Src could be to regulate NMDA channel activity.

NMDA receptor subunits 2A and 2B may be phosphorylated on tyrosine (*20*), and thus Src might regulate NMDA channels by phosphorylating these subunit proteins. Alternatively, Src might phosphorylate other proteins that are in the NMDA channel complex (*15*, *21*). Tyrosine phosphorylation resulted in an increase in P_o, possibly because of an increased probability that the channel will enter long-lived open states. In addition, there is a decreased probability that the channel will be in long shut states. Synaptic NMDA receptor–mediated currents result from single receptor activations that may correspond to clusters or superclusters in single-channel recordings (*22*). The magnitude of the effects of manipulating Src activity on synaptic NMDA currents corresponded to those of the changes in burst and cluster length more closely than to those of the changes in overall P_o. This result is not unexpected given that simulated synaptic NMDA currents change with altered burst and cluster length even without changes in overall P_o (*23*). The changes in single-channel behavior may account for the effects of tyrosine phosphorylation on whole-cell NMDA currents (*3*, *4*), long-term depression in the cerebellum (*24*), and the effects of Src on the synaptic currents reported here. Our findings also indicate that the unique domain of Src may participate in NMDA channel regulation. This domain is not directly involved in catalysis (*25*), and thus it is likely that the sequence containing amino acids 40 through 58 participates in protein-protein interactions necessary for coordinating the phosphorylation of the Src target.

NMDA receptors have been implicated in development, plasticity, and pathology in the CNS (*1*). We postulate that Src, by virtue of its association with and regulation of NMDA receptors, may be important in NMDA receptor–dependent processes. Given that Src and NMDA receptors are widely expressed in the CNS, our results demonstrate a mechanism that may have a general role in regulating excitatory synaptic function in the nervous system.

REFERENCES AND NOTES

1. C. J. McBain and M. L. Mayer, *Physiol. Rev.* **74**, 723 (1994); M. Hollmann and S. Heinemann, *Annu. Rev. Neurosci.* **17**, 31 (1994).
2. L. A. Raymond, C. D. Blackstone, R. L. Huganir, *Trends Neurosci.* **16**, 147 (1993).
3. Y. T. Wang and M. W. Salter, *Nature* **369**, 233 (1994); G. Köhr and P. H. Seeburg, *J. Physiol. (London)* **492**, 445 (1996).
4. Y. T. Wang, X.-M. Yu, M. W. Salter, *Proc. Natl. Acad. Sci. U.S.A.* **93**, 1721 (1996).
5. L. Chen and L.-Y. M. Huang, *Nature* **356**, 521 (1992); S. R. Kelso, T. E. Nelson, J. P. Leonard, *J. Physiol. (London)* **449**, 705 (1992); G. M. Durand *et al.*, *Proc. Natl. Acad. Sci. U.S.A.* **89**, 9359 (1992).
6. H. Thoenen, *Science* **270**, 593 (1995); S. O. Meakin and E. M. Shooter, *Trends Neurosci.* **15**, 323 (1992).
7. J. S. Brugge *et al.*, *Nature* **316**, 554 (1985); R. Martinez, B. Mathey-Prevot, A. Bernards, D. Baltimore, *Science* **237**, 411 (1987).
8. Primary cultures from spinal dorsal horn were prepared from fetal Wistar rats [embryonic day 17 (E17) to E19] as described [M. W. Salter and J. L. Hicks, *J. Neurosci.* **14**, 1563 (1994)]. For single-channel recording, cultures were bathed in extracellular solution composed of 110 mM Na_2SO_4, 10 mM Cs_2SO_4, 25 mM Hepes, 1.3 mM $CaCl_2$, 33 mM glucose, 0.003 mM glycine, and 0.001 mM tetrodotoxin (TTX) (pH 7.35, 310 to 320 mosM). Recording pipettes were made from thin-walled borosilicate glass capillaries (World Precision Instruments, Sarasota, FL) pulled to tips of 1 to 2 μm with 10- to 20-megohm resistance. Pipettes contained the extracellular solution supplemented with 10 μM NMDA and 3 μM glycine. The standard intracellular solution for bathing the cytoplasmic face of the cell membrane contained 140 mM CsCl, 10 mM Hepes, 10 mM 1,2-*bis*(2-aminophenoxy)ethane-*N*,*N*,*N*′,*N*′-tetraacetic acid (BAPTA), 1 mM $CaCl_2$, 2 mM $MgCl_2$, and 4 mM K_2-ATP (pH 7.25, 310 to 320 mosM). Standard intracellular solution but without added K_2-ATP was used where indicated. The intracellular solution was supplemented as required with EPQ(pY)EEIPIA, EPQYEEIPIA, anti-cst1, rabbit IgG, pp60$^{c\text{-}src}$, anti-src1, Src(40–58), or sSrc(40–58) prepared from concentrated (100- to 1000-fold) aqueous stock solutions just before use. The amino acid sequence of sSrc(40–58) was AGSHAPFPSPARAGVAPDA and was created by randomly ordering the sequence of Src(40–58). Chemical sources: EPQ(pY)EEIPIA, EPQYEEIPIA, and sSrc(40–58): J. Bell, Ottawa Regional Cancer Centre, Ottawa; purified recombinant human pp60$^{c\text{-}src}$: Upstate Biotechnology; anti-cst1, anti-src1, and Src(40–58): S. Courtneidge, SUGEN, Redwood City, CA; and BAPTA: Molecular Probes. All other chemicals were from Sigma. Abbreviations for the amino acid residues are as follows: A, Ala; D, Asp; E, Glu; F, Phe; G, Gly; H, His; I, Ile; P, Pro; Q, Gln; R, Arg; S, Ser; V, Val; and Y, Tyr.
9. X. Liu *et al.*, *Oncogene* **8**, 1119 (1993). A concentration of 1 mM was the minimum required to increase Src activity; at concentrations of ≤0.1 mM the peptide had no effect.
10. Single-channel recording and analysis methods, as well as criteria used to ensure that recordings were from NMDA channels, are described elsewhere (*4*). During recordings the holding potential of the patch was +70 mV. For about 75% of channels, the main conductance level was about 50 pS, and for the remainder the main level was about 30 pS. No differences were detected in effects in the two populations, and thus data from the two groups were pooled. We determined P_o, open times, and shut times off-line using a 50% crossing threshold. Channel activity at 5 to 10 min after the start of compound application was compared with that for a similar period immediately preceding the application. Distributions of dwell times were fitted with the sum of multiple exponentials by Levenberg-Marquardt least-squares method. The usefulness of adding exponential components was assessed by means of an F test [Y. De Koninck and I. Mody, *J. Neurophysiol.* **71**, 1218 (1994)] and by visual inspection. Groupings of openings into bursts, clusters, and superclusters [A. J. Gibb and D. Colquhoun, *J. Physiol. (London)* **456**, 143 (1992)] were determined according to critical times (t_c), where $t_c = 1 - e^{-t_c/t_s} = e^{-t_c/\tau_m}$ [D. Colquhoun and B. Sakmann, *J. Physiol. (London)* **369**, 501 (1985)]. Values of t_c (mean ± SEM) for the bursts, clusters, and superclusters were 3.3 ± 0.4, 50.7 ± 8.0, and 500 ± 130 ms, respectively. Synaptic Toolbench software (Y. DeKoninck, McGill University) was used to analyze the bursts, clusters, and superclusters.
11. X.-M.Yu, R. Askalan, G. J. Keil II, M. W. Salter, data not shown.
12. S. Roche, M. Koegl, M. V. Barone, M. F. Roussel, S. A. Courtneidge, *Mol. Cell. Biol.* **15**, 1102 (1995).
13. S. Roche, S. Fumagalli, S. A. Courtneidge, *Science* **269**, 1567 (1995).
14. Spinal cord membranes were prepared from fetal rats (E17 to E19) with methods adapted from Sheng *et al.* [M. Sheng, M.-L. Tsaur, Y. N. Jan, L. Y. Jan, *Neuron* **9**, 271 (1992)]. Membrane proteins were solubilized under nondenaturing or denaturing conditions. Nondenaturing conditions: ice-cold 50 mM tris-HCl (pH 7.6) containing 150 mM NaCl, 1% igepal ca630 0.5% sodium deoxycholate, 0.1% SDS, 2 mM EDTA, 1 mM sodium orthovanadate, and the protease inhibitors pepstatin A (20 μg/ml), leupeptin (20 μg/ml), aprotinin (20 μg/ml), and phenylmethylsulfonyl flouride (1 mM). Denaturing conditions: boiling in 1% SDS followed by fivefold dilution with 50 mM tris-HCl (pH 7.6) containing 190 mM NaCl, 1.25% Triton X-100, 1 mM sodium orthovanadate, 6 mM EDTA, and the protease inhibitors listed above. Solubilized proteins (300 μg) were centrifuged at 14,000*g* to remove insoluble material and then incubated with anti-NR1 (5 μg) or anti-Src (1:100 dilution) or with control, nonspecific IgG (5 μg) overnight at 4°C. Immune complexes were isolated by the

addition of 50 μl of protein G–Sepharose beads followed by incubation for 4 hours at 4°C. Immunoprecipitates were then washed five times with lysis buffer, resuspended in 2× Laemmli sample buffer, and boiled for 5 min. The samples were subjected to SDS–polyacrylamide gel electrophoresis (PAGE) (10% gel) and transferred to a nitrocellulose membrane. Analysis was performed by repeated stripping of the membrane and successive probing with anti-NR1 (5 μg), anti-Src (1:500 dilution), or anti-Kv3.1 (1:4000 dilution). Sources of antibodies: anti-NR1 (mouse monoclonal anti-NMDAR1): Pharmingen; anti-Src (monoclonal antibody 327): J. Bolen, DNAX, Palo Alto, CA; nonspecific mouse IgG, Calbiochem, San Diego, CA; and anti-Kv3.1 (rabbit antisera): T. Perney, Rutgers University.

15. M. Sheng, J. Cummings, L. A. Roldan, Y. N. Jan, L. Y. Jan, *Nature* **368**, 144 (1994).
16. T. M. Perney and L. K. Kaczmarek, *Semin. Neurosci.* **5**, 135 (1993).
17. Whole-cell recordings were made from cultured dorsal horn neurons as described [Y. T. Wang and M. W. Salter, *Nature* **369**, 233 (1994)]. The cultures were bathed in an extracellular solution composed of 140 mM NaCl, 5.4 mM KCl, 33 mM glucose, 1.3 mM $CaCl_2$, 10 mM Hepes, 0.001 mM TTX, 0.01 mM bicuculline, and 0.01 mM strychnine (pH 7.25, 310 to 320 mosM). The recording pipette (4- to 7-megohm resistance) contained intracellular solution composed of 90 mM Cs_2SO_4, 35 mM CsOH, 1.3 mM $CaCl_2$, 11 mM EGTA, 10 mM Hepes, and 4 mM MgATP (pH 7.25, 285 to 305 mosM). EPQ(pY)-EEIPIA, EPQY-EEIPIA, anti-src1, Src(40–58), or sSrc(40–58) were added to the intracellular solution as required. Whole-cell currents were recorded with an AxoPatch 1D amplifier (Axon Instruments) that were digitized (33 KHz) and stored on videotape. Detection and analysis of mEPSCs was done off-line (Synaptic Toolbench) after alignment of their rising edges. Mean mEPSCs contained at least 30 traces. Traces with more than one mEPSC per 200-ms recording period, typically 1 to 5% of the total, were not included in the analysis. Under the present recording conditions, spontaneously occurring mEPSCs were observed in most cells. In all cells, the frequency of the mEPSCs was facilitated by the local application of hypertonic sucrose solution. The slower component of the mEPSCs was blocked by D,L-2-amino-5-phosphonovaleric acid and the fast component was abolished by 6,7-dinitroquinoxaline-2,3(1H,4H)-dione (DNQX, 10 μM).
18. J. M. Bekkers and C. F. Stevens, *Nature* **341**, 230 (1989).
19. S. G. N. Grant *et al.*, *Science* **258**, 1903 (1992); P. Soriano, C. Montgomery, R. Geske, A. Bradley, *Cell* **64**, 693 (1991).
20. I. S. Moon, M. L. Apperson, M. B. Kennedy, *Proc. Natl. Acad. Sci. U.S.A.* **91**, 3954 (1994); L. F. Lau and R. L. Huganir, *J. Biol. Chem.* **270**, 20036 (1995).
21. H.-C. Kornau, L. T. Schenker, M. B. Kennedy, P. H. Seeburg, *Science* **269**, 1737 (1995); M. D. Ehlers, S. Zhang, J. P. Bernhardt, R. L. Huganir, *Cell* **84**, 745 (1996).
22. B. Edmonds and D. Colquhoun, *Annu. Rev. Physiol.* **5**, 495 (1995).
23. D. Lieberman and I. Mody, *Nature* **369**, 235 (1994) .
24. A. R. Boxall, B. Lancaster, J. Garthwaite, *Neuron* **16**, 805 (1996).
25. G. Superti-Furga and S. A. Courtneidge, *Bioessays* **17**, 321 (1995).

26. We thank S. Courtneidge, J. Bolen, T. Perney, and R. Wenthold for antibodies; J. F. MacDonald, T. Pawson, and J. C. Roder for critical comments on the manuscript; and Y. De Koninck for software used in analysis. Supported by a grant from the Medical Research Council (MRC) of Canada (M.W.S.) and by the Nicole Fealdman Memorial Fund. M.W.S. is an MRC Scholar, X.-M.Y. is supported by a Fellowship from the Spinal Cord Research Foundation of the Paralyzed Veterans of America, and R.A. is a Fellow of the Rick Hansen Man in Motion Foundation. We thank J. L. Hicks for preparing and maintaining cell cultures and for technical assistance.

2 August 1996; accepted 22 November 1996

Positive Selection of T Cells Induced by Viral Delivery of Neopeptides to the Thymus

Naoko Nakano, Ronald Rooke, Christophe Benoist, Diane Mathis

The relation between an antigenic peptide that can stimulate a mature T cell and the natural peptide that promoted selection of this cell in the thymus is still unknown. An experimental system was devised to address this issue in vivo—mice expressing neopeptides in thymic stromal cells after adenovirus-mediated delivery of invariant chain–peptide fusion proteins. In this system, selection of T cells capable of responding to a given antigenic peptide could be promoted by the peptide itself, by closely related analogs lacking agonist and antagonist activity, or by ostensibly unrelated peptides. However, the precise repertoire of T cells selected was dictated by the particular neopeptide expressed.

Mature T lymphocytes display a biased repertoire of T cell receptors (TCRs), enriched for those that can recognize foreign antigens presented by the animal's own major histocompatibility complex (MHC) molecules and largely purged of those capable of seeing self-antigens in the context of self-MHC molecules (*1*). These biases reflect positive and negative selection processes that take place in the thymus, both controlled by interactions between the TCRs on differentiating thymocytes and the MHC molecules on stromal cells. Positive selection is of particular interest because it shapes the T cell repertoire to deal with antigens not encountered until some time in the future, or even never. Other than that MHC molecules are involved, the precise nature of the ligands that promote positive selection remains undefined.

One system used to address this issue relies on the addition of peptides to fetal thymic organ cultures (FTOCs) derived from mouse strains carrying mutations that interfere with peptide loading and surface display of MHC class I molecules (*2–10*). These studies agreed that peptides are required for positive selection, but disagreed on the nature of the most effective peptides and on their precise role. In addition, this approach has limitations: First, the FTOC systems can give an indication of which peptides are capable of enhancing the selection of a given TCR, but do not address those actually responsible for selection; second, as discussed (*11*, *12*), such systems create a situation in which thymocytes are exposed to few MHC molecules heavily loaded with a single peptide, unlike the natural condition where many MHC molecules carry a heterogeneous mix of peptides.

An alternative approach allows the identification of T cells selected in vivo on a defined peptide. Mouse strains were engineered that express MHC class II molecules loaded with a single peptide—either by introduction of a transgene that encodes a class II chain covalently linked to a particular peptide (*13*) or by generation of a null mutation of the H-2M gene, resulting in class II molecules filled with a peptide derived from the invariant chain (Ii) (*14*, *15*). Surprisingly, results from these studies were largely in agreement: A single peptide promoted selection of a large number of T cells (*13–15*) with a diverse repertoire of TCRs (*13*, *14*). This approach has overcome one of the criticisms of the experiments that use FTOCs but remains susceptible to the second in that these systems produce a situation in which low (*13*) or normal (*14*, *15*) amounts of MHC molecules are loaded with essentially one peptide.

To surmount both limitations, we injected mice intrathymically (i.t.) with an adenovirus vector that directs expression of a peptide of choice (neopeptide) in a form that favors its presentation by MHC molecules on thymic stromal cells. The vector is a nonreplicating derivative of the Ad5 strain, bearing a deletion of the critical E1a and b region (Fig. 1A), which was replaced by a cassette that controls expression of a given cDNA in cells that normally express MHC class II molecules (Fig. 1B). Intrathymic injection of adenoviruses carrying cDNAs within this cassette (*16*) results in measurable protein expression 10 days later, remaining detectable for about 4 weeks. Proteins are expressed in amounts similar to those of endogenously encoded MHC class II molecules and occur primarily in the class II–positive epithelial cells of the cortex and medulla. Expression is confined to an area about 3 to 20% of the injected lobe, does not "spread" to an adjacent uninjected lobe, and is not detectable in the peripheral lymphoid organs. Thus, this system permits one to influence thymic selection quite specifi-

Institut de Génétique et de Biologie Moléculaire et Cellulaire (INSERM, CNRS, Université Louis Pasteur), 1 rue Laurent Fries, 67404 Illkirch, C.U. de Strasbourg, France.